Journal of Applied Electrochemistry **34**: 705–714, 2004.

Effects of Nafion® dehydration in PEM fuel cells

M. CIUREANU
Ecole Polytechnique Montreal, Engineering Physics Department PO 6079 succ. Centre-ville, Montréal, Québec, H3C 3A7, Canada (Mariana.Ciureanu@polymtl.ca)

Received 9 December 2003; accepted in revised form 14 January 2004

Key words: electrochemical impedance spectroscopy, Nafion dehydration, proton exchange fuel cells

Abstract

The current dependence of the ohmic resistance of Nafion membranes was examined with different types of humidification: cathodic (ChAd), anodic (CdAh), anodic and cathodic (ChAh) and no humidification at all (CdAd). Data show that for stacks with humidified cathodes (ChAd and ChAh), the resistance is small and relatively insensitive to the presence of the anodic humidification. On the contrary, for stacks with non-humidified cathodes (CdAh and CdAd), the membrane resistance is high and strongly dependent on current and anodic humidification. The kinetics of membrane dehydration was examined by recording the galvanostatic transients of the stack voltage and resistance, after removing the humidification. It was found that the changes in the ohmic resistance $\Delta R_\Omega(t)$, although significant, cannot explain entirely the observed decay of the stack voltage. To account for the difference, an additional resistive term is introduced $\Delta R_p(t)$. Explicit equations were found for the time and current dependence of the two resistive terms $\Delta R_\Omega(t)$ and $\Delta R_p(t)$ after humidification removal. A tentative explanation for the new resistive term was provided using electrochemical impedance spectroscopy (EIS). EIS data obtained at low overpotential show that dehydration of the Nafion present in the cathode catalytic layer results in an increase of the polarization resistance; the apparent deactivation of the cathode electrocatalyst appears to be due to a decrease of the electrochemically active surface area.

List of symbols

R_Ω	total stack resistance
r_s	area resistance
r_m	area resistance of the Nafion membrane
r_n	value of the steady state area resistance of the membrane after long term operation ($t = \infty$) in the absence of cathode humidification.
r_{mo}	value of the the steady state area resistance of the membrane resistance in the presence of humidification
k	rate constant for the increase of the membrane resistance due to dehydration
$\tau = 1/k$	time constant for the membrane dehydration
ΔR_p	increase of the total polarization resistance due to the dehydration of Nafion in the catalytic layer
k'	rate constant for the increase of the polarization resistance due to the dehydration of Nafion in the catalytic layer
$\tau' = 1/k'$	time constant for the increase of the polarization resistance

1. Introduction

Proton exchange membrane fuel cells (PEMFC) are promising power sources since they offer a highly efficient and environmentally friendly solution for energy conversion. In these devices the organic proton exchange membrane plays the dual role of electrolyte and gas separator. Nafion, a perfluorinated polymer from DuPont, is the most widely used membrane material owing to its high ionic conductibility and excellent chemical resistance. Because the ionic conductibility of Nafion is high only in the wet state and deteriorates as soon as it starts to dry, water management to protect it from drying is a major concern during fuel cell operation. This subject has attracted considerable research effort in recent years, aimed to provide a better understanding of the water uptake characteristics of Nafion exposed to vapor or liquid [1–3], the transport of ions [4, 5] and the properties of water transport across the membrane [6–10]. The conductivity of Nafion was extensively studied in *ex situ* experiments performed by a.c. impedance [1, 3, 11, 12], or current pulse techniques [4], in various environments: liquid water, 1 M H_2SO_4 and water vapour. Data obtained are rather scattered, with values ranging from 0.05 to 0.23 S cm^{-1}, which reflects the important role of working conditions, membrane pretreatment and experimental conditions. A detailed analysis of the impact of those factors on the

proton conductivities of Nafion was made by Sade et al. [13]. These authors also demonstrate that the conductibility decreases for thinner membranes.

From the practical point of view, the most interesting data are those obtained from *in situ* FC experiments [13–17]; the main topics of these papers are the conductivity dependence on membrane thickness and current. Data on the current dependence are apparently contradictory: Buchi et al. [14, 15] reported an increase of the membrane resistance with increasing current for membranes thicker than 120 μm, and essentially constant values from membranes with a thickness in the 60–120 μm. Watanabe et al. [17] performed experiments in anode-humidified fuel cells, with thin layers of recast Nafion and found a decrease of the membrane resistance with increasing current density. The apparent discrepancy of those results can be reconciled if the current dependence of the conductivity is different, depending on the membrane thickness.

There are still a series of unanswered problems regarding the resistance of the Nafion membrane under various conditions of fuel cell operation. The first of these would be a direct comparison of the current dependence of the membrane resistance, measured on the same system, in different conditions of humidification: only anodic, only cathodic, both anodic and cathodic, or no humidification at all. Such information could provide an answer to a question with great practical significance: since the anodic part of the membrane is known to be drier than the cathodic part, is the air humidification replaceable by the humidification of fuel? A second question of practical relevance is the rate at which the membrane dehydrates, once the humidification is removed, as well as the current dependence of this rate. A third question to be answered is whether the dehydration of the membrane is the sole factor responsible for the voltage decay after humidification removal, or there is also a contribution due to the dehydration of the Nafion present in the catalytic layers.

In an attempt to provide information to the above questions, this paper presents *in situ* measurements on small FC stacks with thin Nafion membranes (30 μm). Data will be provided for cells of the size normally used for systems in the 5–10 kW range, operated at current densities from zero to 0.4 A cm^{-2}.

2. Experimental details

The fuel cell tested was a stack of five cells, with machined graphite bipolar plates and an active geometric surface area ($A = 256$ cm^2). Each cell had a separate cooling plate, which enabled regulating the stack temperature with an accuracy of ± 1 °C, using a thermostated water bath. The temperature of the experiments was 52 $\pm$ 1 °C. The MEA were from Gore Associates (Primea 5561) with carbon-supported Pt/Ru catalyst and Carbel as diffusion medium. The Nafion membranes had a thickness of (30 $\pm$ 2) μm in dry state.

The electrodes were supplied with pure hydrogen (the anode) and air (the cathode) at atmospheric pressure. The inlet airflow was changed with the current, to correspond to a constant stoichiometry of 4; this value, higher than usually employed in fuel cell experiments, was selected in order to insure a complete removal of the water produced in the cathode compartment. The hydrogen flow rate was changed according to $f_a = 1.1 + 1.1\, f_{st}$, where f_{st} is the stoichiometric flow rate in litres per minute.

Humidification of air and fuel was made using Permapure humidifiers. The temperature of water and gases at the stack inlet/outlet was measured using thermocouples.

The experiments were performed in galvanostatic mode, using a 1 kW test station manufactured by Fuel Cell Technologies. The test station enabled determining *in situ* the ohmic resistance of the stack, using the interruption technique [14, 15]. Resistance data thus obtained were compared with those from electrochemical impedance spectroscopy (EIS) experiments and were found to be in a satisfactory agreement.

The a.c. impedance spectra were recorded using a Schlumberger 1250 frequency response analyser, controlled by a PAR 273A potentiostat–galvanostat (EG&G Instruments). The impedance spectra were measured in the constant voltage mode by sweeping frequencies over the 0.015 Hz–65 kHz range, and recording ten points/decade. The modulating voltage was 15 mV. To minimize contact resistances, measurements were made in a four-probe arrangement. The impedance spectrum in the high frequency range shows an inductive behaviour, characteristic to the experimental set-up. To avoid complications resulting from these characteristics, we have limited the high frequency range to 1 kHz.

3. Results

3.1. *Dependence of the membrane resistance on current and type of humidification*

To estimate the conductivity of the Nafion membrane from stack resistance data, the relative contributions of various terms to the total ohmic resistance of the cell were determined.

The ohmic resistance R_Ω of the stack with N cells can be expressed as a sum of contributions from the uncompensated contact resistance R_c (wires and connectors) and the ohmic resistances of the cell components: the resistance of the membrane (R_m), the catalyst layer (R_{cat}), the backing (R_{bac}), the endplates (R_{ep}) and the contacts between the membrane/catalyst layer ($R_{m/cat}$), catalyst layer/backing $R_{cat/back}$, and backing/endplates ($R_{back/ep}$). Among those terms, R_m and $R_{m/cat}$ are ionic resistances, while the remaining terms are electronic resistances:

$$R_\Omega = R_c + N(R_m + R_{cat} + R_{back} + R_{ep} + 2R_{m/cat} + 2R_{cat/back} + 2R_{back/ep}) = R_c + NR_s \quad (1)$$

To separate R_s from R_c, we determined the resistance of the stack containing different numbers (N) of cells, in an experiment in which one of the voltage probes was maintained constant and the other was successively switched between cells 1 to 5. The value of $R_\Omega = R_t + N\ R_{si}$ (where R_{si} is the resistance of a single cell) was represented as a function of N. The linearity of the data showed that the five cells had equal resistance. The slope of the straight line thus obtained provided the resistance of a single cell R_{si}, while the ordinate yielded the value of the contact resistance $R_c = 2.46$ mΩ. The values R_{si} were thus used to evaluate the area resistance $r_s = R_{si}S$ (where S is the geometrical area $S = 256$ cm^2). The r_s values cannot be used to determine directly the membrane conductivity, since they contain non-negligible contributions from the resistance of the bipolar plates and gas diffusion medium; a separate evaluation of those terms in experiments without membranes resulted in values in the 0.05–0.07 mΩ cm^2. Since these values are 40–60% of the measured area resistances in humidified conditions, our study will be limited to discussing r_s, instead of membrane conductivity. Among the resistive components contributing to the value of r_s, it is only the Nafion resistance that is influenced by the humidification.

Figure 1 presents the dependence of the ohmic resistance of the stack on the current, as measured for different types of humidification: AdCd (anode dry, cathode dry), AdCh (anode dry, cathode humidified), AhCd (anode humidified, cathode dry), AhCh (both anode and cathode humidified). This Figure clearly shows that there are two distinct behaviours, depending on the humidification of the cathode: for cases AdCh and AhCh, the resistance is low and almost constant over the investigated current range. For cases AdCd and AhCd (with non-humidified cathodes), the resistance is high, and shows a significant decrease with increasing current; the decrease is more significant for AhCd, which at low currents has a resistance close to AdCd, while at high current it approaches values obtained for AdCh. The above data clearly demonstrate that the anodic humidification and cathodic humidification are not equivalent and that optimal membrane conductibility cannot be obtained with anodic humidification only.

The dependence of the membrane resistance on current and humidification type depends on the distribution and transport of water in the membrane. The net amount of water transported across the membrane is the result of two processes directed in opposite directions: the electroosmotic drag and the back diffusion. In our previous paper [18], it was shown that if the global concentration of water in the cathodic compartment (resulting both from the electrochemical process and the humidified air stream) is higher than the concentration of water that can be removed as saturated vapour, then liquid water tends to accumulate in the cathodic compartment; the result is that the concentration of water at the Nafion surface attains the limiting value c_o. This case applies for fuel cells with humidified cathodes (AdCh and AhCh), which explains why, in such cases, the net water flux through the membrane is directed from the cathode to the anode [18]. As long as the net amount of water transported from the cathode to the anode is sufficient to compensate for the evaporation at the anode interface, the resistance of the membrane remains low. Since the water concentration at the cathode/membrane interface cannot exceed the limiting

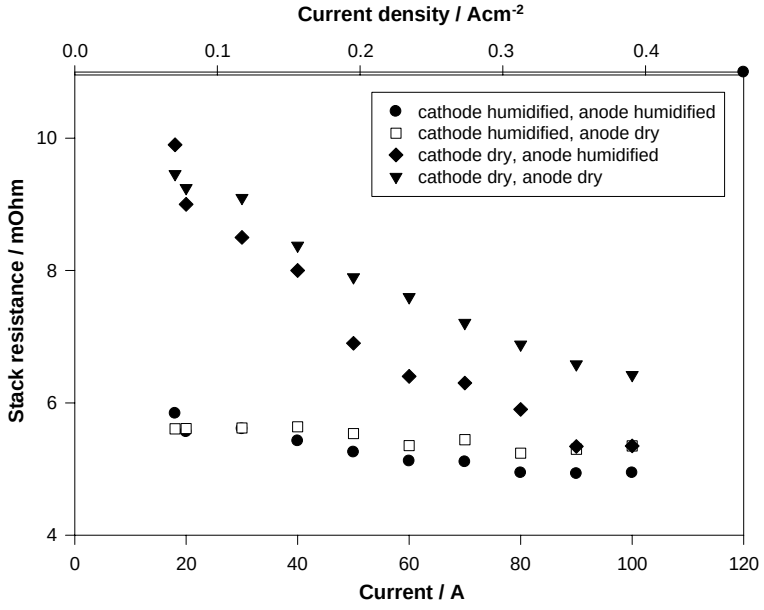

Fig. 1. Ohmic resistance of the stack as a function of current for different humidification types.

value, the increase of current results only in accumulation of more liquid at the interface, so that no major variations are expected for the resistance as the current changes.

If the cathode is not humidified (cases AhCd and AdCd), the water concentration at the cathode/membrane interface is smaller than c_o and increases with the water produced electrochemically, that is, with the current. In this case, the cathodic side of the membrane contributes to a non-negligible extent to the resistance. The water concentration gradient across the membrane is also considerably smaller (particularly for thin membranes) than in the preceding cases (AdCh or AhCh), so the amount of water transported to the anode by back diffusion is lower. Both effects are responsible for the high resistance observed at low currents for AdCd.

For AhCd, at low currents the sense of the net transport across the membrane is directed from anode to cathode [18]; in this case, the anode side of the membrane is still dehydrated, so that the humidification of the anode produces only a moderate decrease in resistance for AhCd with respect to AdCd. On the other side, the effect of current increase is a major one, since it determines a reversal of the sense of transport for $i > 0.25$ A cm^{-2}. This explains the fact that at high current, AhCd behaves similarly to a system with humidified cathode.

3.2. *Kinetics of dehydration*

The membrane dehydration experiments included recording the resistance transients after humidification removal at constant current and stack temperature. Figure 2 presents four possible situations, recorded at a constant current of 60 A ($i = 0.234$ A cm^{-2}): curves (a) and (b) present the cases when the stack initially had both anodic and cathodic humidification (AhCh): the transient was recorded after cutting off humidification at the anode (a), or at the cathode (b). Curves denoted by (c, d) present the effect of humidification interruption when the stack initially had only the humidified compartment: cathode for (c), or anode for (d). It may be seen that the effect of removal is a major one for cathodic humidification and a relatively unimportant one for anodic humidification.

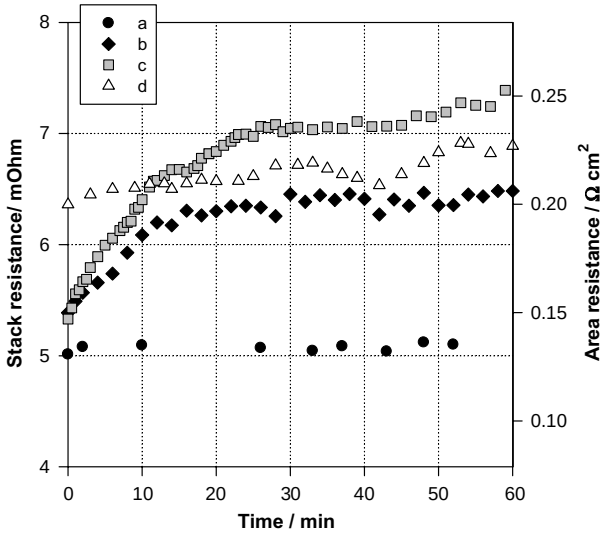

Fig. 2. Transients of the ohmic resistance at constant current ($I = 60$ A): (a) after cutting off the anode humidification. Initial state ChAh; (b) after cutting off the cathode humidification. Initial state ChAh; (c) after cutting off the cathode humidification. Initial state ChAd; and (d) after cutting off the anode humidification. Initial state CdAh.

To provide information on the kinetics of the MEA dehydration process after humidification removal, we considered in more detail the cases denoted by (c) and (d), in which the stack had initially only one type of humidification: cathodic (c) or anodic (d).

3.2.1. *Effect of cutting off the cathode humidification*

Before starting the experiment, the stack was left to equilibrate at 50 A and 52 °C, with cathodic humidification; the temperature of the humidified air at the stack inlet was 42 °C. The humidification conditions were selected to be similar to those used in practical applications for medium and large size PEM FC stacks, that is, with a temperature of humidification lower than the temperature of the stack, which results in a relative air humidity lower than 100%. If the air humidity were 100% at the stack inlet, the excess water produced electrochemically would overflow the cathode [18].

After 30 min, the current was switched to the working value and the stack was left to equilibrate with continuous humidification for another 15 min. Subsequently, the cathodic humidification was cut and the change of the voltage and resistance were followed as a function of time for 40–60 min. From Figure 3(a) it may be observed that the stack resistance increases rapidly in the first minutes after humidification removal and after 40–60 minutes, it levels off to an almost constant value.

The transients presented in Figure 3(a) can be used to provide information on the kinetics of membrane dehydration. The rate of increase of the membrane resistance can be expressed as

$$\frac{dr_m}{dt} = -k(r_m - r_n) \tag{3}$$

where r_n is higher than the initial value of the resistance in the presence of humidification by a constant value δ:

$$r_m(t = 0) = r_{mo} \tag{4}$$

$$r_n \equiv r_m(t = \infty) = r_{mo} + \delta \tag{5}$$

Integrating Equation 3 with the boundary conditions (4) and (5) gives the time dependence of the resistance increase:

$$r_m(t) = r_{mo} + \delta[1 - \exp(-kt)] \tag{6}$$

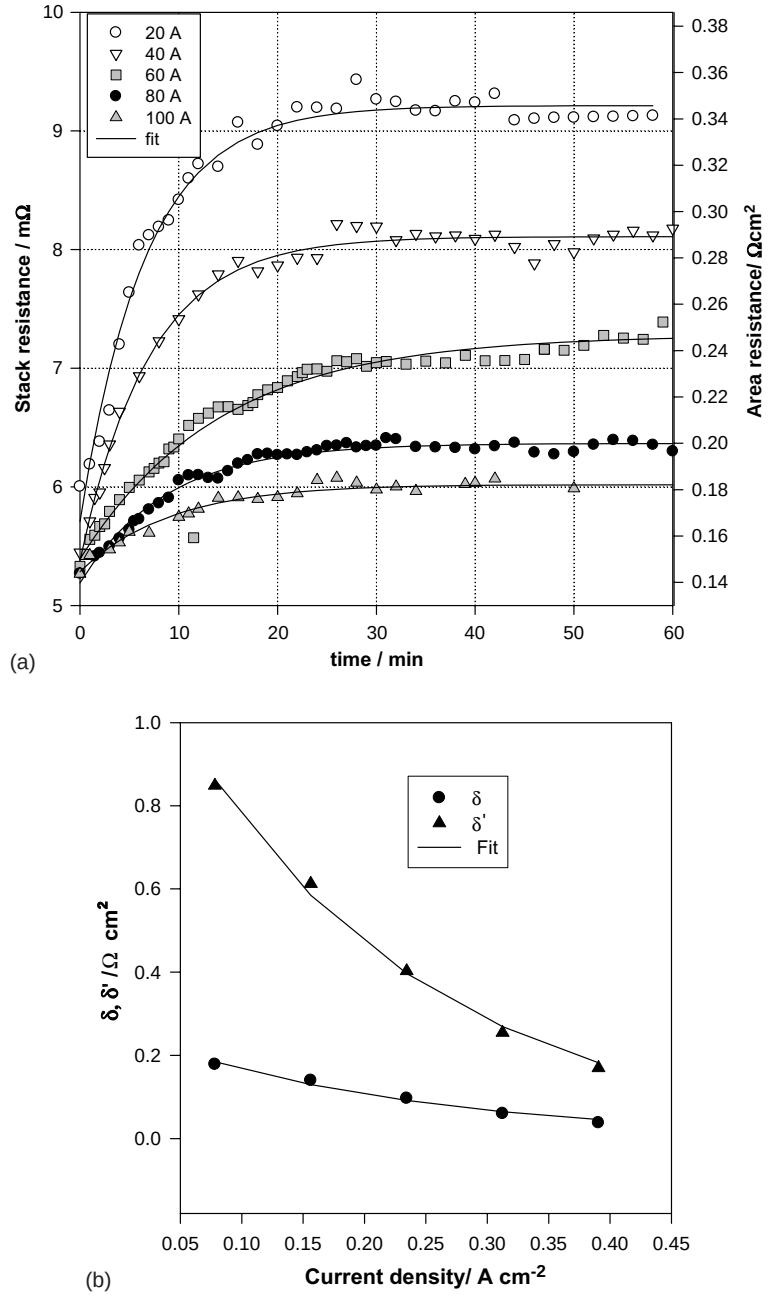

Fig. 3. (a)Transients of the ohmic resistance after interruption of the cathodic humidification. Legend specifies the stack current. Initial state ChAd. (b) Current dependence of the parameters δ and δ'.

Equation 6 was used to fit the experimental transients of Figure 3(a) to obtain the values of the parameters in Equation 6. Since the resistance of the current collectors and carbon paper are not influenced by water exposure, they are included in the time-independent term, so that the experimental values of the area resistance are identical with $\Delta r_m = r_m(t) - r_{mo}$. Figure 3(a) presents a comparison of the experimental data (points) and the fitted dependences (lines). The value of the rate constant k was found to be $k = 0.118 \pm 0.04$ min^{-1}.

The values of δ are a function of the current density, as seen from Figure 3(b). The data could be fitted to an exponential relationship:

$$\delta = a \exp(-i/i_m) \tag{7a}$$

with the parameters $a = 0.26\ \Omega\ \text{cm}^2$ and $i_m = 0.22\ \text{A cm}^{-2}$.

Combining Equations 6 and 7(a), gives the time and current-dependence of the ohmic resistance after removing the cathode humidification:

$$\Delta r_m(t) = a \exp(-i/i_m)[1 - \exp(-t/\tau)] \tag{7b}$$

3.2.2. *Effect of cutting off the anode humidification*

A similar series of experiments was performed on the stack initially humidified only on the anodic side. Before

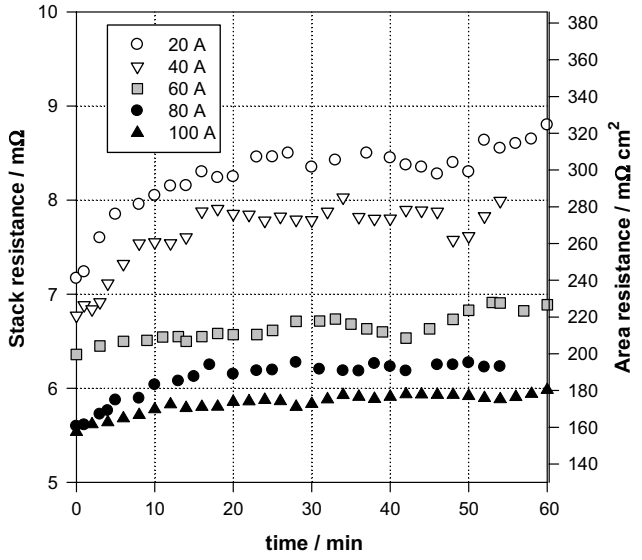

Fig. 4. Transients of the ohmic resistance after interruption of the anodic humidification. Legend specifies the stack current. Initial state CdAh.

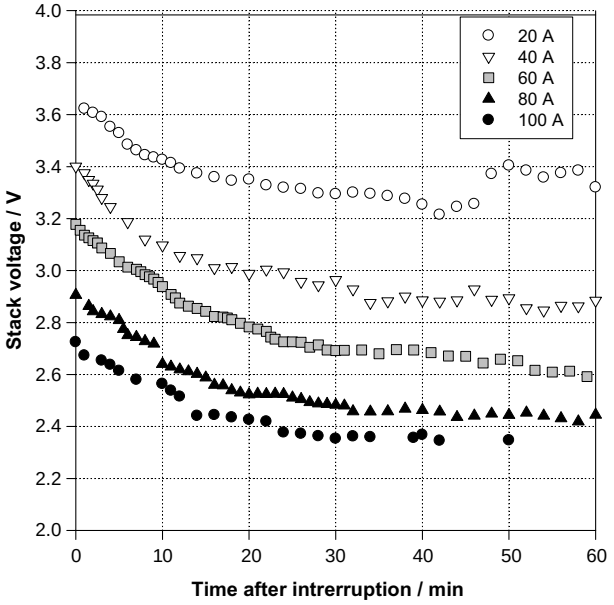

Fig. 5. Transients of the stack voltage after interruption of the cathodic humidification. Legend specifies the stack current. Initial state ChAd.

starting the experiment, the stack was left to equilibrate at the working current and 52 °C, with anodic humidification; the temperature of the humidified hydrogen at the stack inlet was 42 °C. After 30 min, the anodic humidification was cut off and the change in voltage and resistance were followed as a function of time for 40–60 min.

The transients obtained for the ohmic resistance R_Ω at several currents are presented in Figure 4. Inspection of those figures reveals several differences with respect to those obtained in the previous case: (a) the initial values of the ohmic resistances are higher than for humidified cathode; (b) the overall increase in time is considerably smaller; and (c) the transients at low and high currents have different patterns: those at 20 A and 40 A have an appearance close to that observed previously with removal of cathodic humidification. At the highest currents (I = 60–100 A), the transient shows small, but reproducible, oscillations. The presence of the oscillations prevented us from performing a systematic evaluation of parameters, as done in the previous case.

3.3. *Effect of Nafion dehydration in the cathode catalytic layer*

Although changes of the membrane resistance after interruption of the cathode humidification are relatively important, the corresponding ohmic drop cannot account entirely the for the observed voltage decay. The voltage transients obtained simultaneously with the resistance transients are presented in Figure 5 for five values of the current. Figure 6 presents a comparison between the voltage transient $E(t)$ at I = 60 A and the calculated values of the function:

$$E'(t) = E(0) - I\,[R_\Omega(t) - R_\Omega(0)] = E(0) - I\Delta R_\Omega \qquad (8)$$

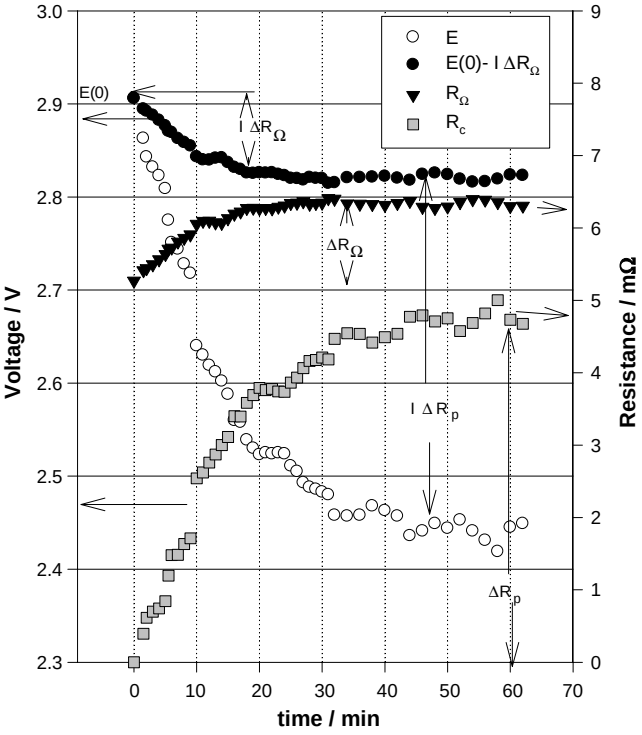

Fig. 6. Voltage transient $E(t)$ after interruption of the cathodic humidification (I = 60 A). The transients $R_\Omega(t)$ and calculated $\Delta R_p(t)$, as well as the function $E(0) - I\Delta R_\Omega$ are also presented.

Increase in ohmic drop $I\Delta R_\Omega$ accounts for only a small fraction of the observed voltage decay. The system behaves as if an additional resistance change appears:

$$\Delta R_p = \frac{E(t) - E'(t)}{I} \qquad (9)$$

Figure 6 shows that the values of ΔR_p are significantly higher than those of ΔR_Ω. The additional increase in area resistance Δr_p was found to obey a time dependence similar with that of Δr_m.

$$\Delta r_p = \delta'[1 - \exp(-k't)] \quad (10)$$

Since the resistance of the current collectors and carbon paper are not influenced by water exposure, Δr_p should be assigned to a dehydration effect, namely that of the Nafion in the catalytic layer. The presence of the polymer in the catalytic layer is required in order to insure continuity of the proton paths from the membrane to the active site. Dehydration of the Nafion in this layer is expected to occur at a lower rate than that of the membrane, since it is closer to the water-generating sites. This is confirmed by the experimental and fitted time dependences of Δr_p, presented in Figure 7 from which the rate constant was determined to be $k' = 0.061 \pm 0.01\ \text{min}^{-1}$, a value lower than that found for k. The values δ' are compared in Figure 3(b) with those obtained previously for δ. Time and current dependence of Δr_p are represented by

$$\Delta r_p = a' \exp\left(\frac{-i}{i'_m}\right)\left[1 - \exp\left(\frac{-t}{\tau'}\right)\right] \quad (11)$$

where the values obtained from the fit, $a' = 1.272\ \Omega\ \text{cm}^2$ and $\tau' = 15$ min, are higher than the corresponding values obtained for the membrane resistance, while the value $I'_m = 0.22\ \text{A cm}^{-2}$ is almost equal to that obtained for i_m.

3.4. *EIS experiments*

To provide a better understanding of the causes determining the appearance of the new resistive term, EIS spectra of the stack were recorded before and at different intervals after removing the cathodic humidification (Figure 7). As discussed previously, these spectra provide information only about the cathode impedance, since anodic contributions are extremely small [19]. The spectra were recorded under potentiostatic conditions, with $V_{bias} = 4.5$ V, which corresponds to an average cell voltage of 0.9 V. This value was selected to be close to the open circuit cell voltage ($E_{OCV} = 0.925$ V) to avoid mass transport effects. At lower cell voltages (high overvoltages), the EIS spectrum generally consists of two loops, with the low frequency loop due to the slow diffusion of air in the gas diffusion medium [19]. At potentials close to OCV, the spectrum contains only the high frequency loop and the changes observed in the EI spectra are due to ohmic and charge transfer effects [19].

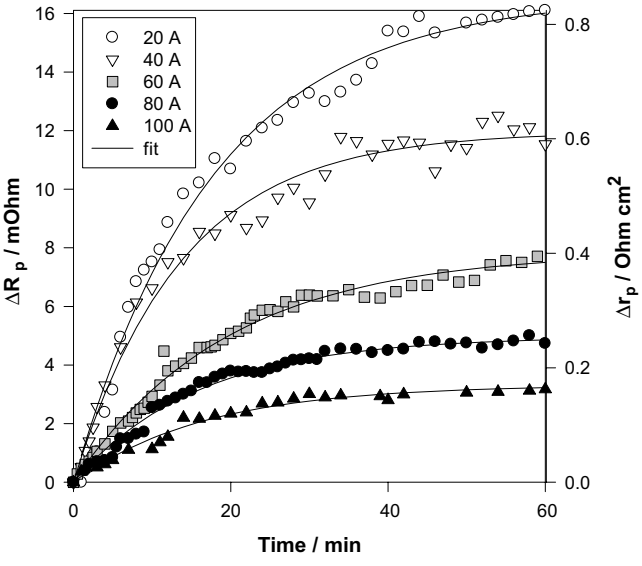

Fig. 7. Transients of ΔR_p after interruption of the cathodic humidification. Legend specifies the stack current. Initial state ChAd.

Figure 8(a) and (b) present the spectrum of the stack (Nyquist and Bode plots) with cathodic humidification (case AdCh), as well as spectra recorded at $t = 5$, 10, 20, 30, 40, 50 and 60 min after removing the humidification. The high frequency limit of the spectrum represents the ohmic resistance of the membrane; while the values increase in time, changes are too small to be observed on the scale of the graph. In Contrast, it may be seen that the diameter of the semicircle shows a considerable increase; this diameter provides information on the polarization resistance. The value of the latter will be denoted R'_p to distinguish it from that obtained in galvanostatic conditions. Values of R'_p, as well as those of the double layer capacitance of the cathode C_{dl}, were obtained by fitting the experimental EI spectra to an equivalent circuit containing a series combination of R_Ω with a parallel circuit (R'_p, C_{dl}). The values obtained for R'_p and C_{dl} (values for the entire stack) at different time intervals after interruption of the cathodic humidification are presented in Figure 9.

The increase of R'_p can be used to provide information about the changes produced by dehydration in the cathode catalytic layer. At constant overpotential, the area resistance r'_p is related to the apparent value of the charge transfer resistance $(r^o_p)_{app}$ by the simple relationship [19]:

$$r'_p = (r^o_p)_{app} \exp\left(\frac{-\eta}{b}\right) \quad (12)$$

Here η is the cathode overpotential and b is the Tafel slope $b = RT/(\alpha n F)$, where n is the number of electrons transferred in the rate-determining step and α is the charge transfer coefficient. Since the potential applied is very close to the OCP, both mass transport and ohmic overpotentials are very small, so that the overpotential is determined by the charge transfer term.

In the present experiments η is constant, so that the observed changes of r'_p are due to $(r^o_p)_{app}$. The latter value is related to the apparent exchange current density $(i^o)_{app}$ by the simple equation:

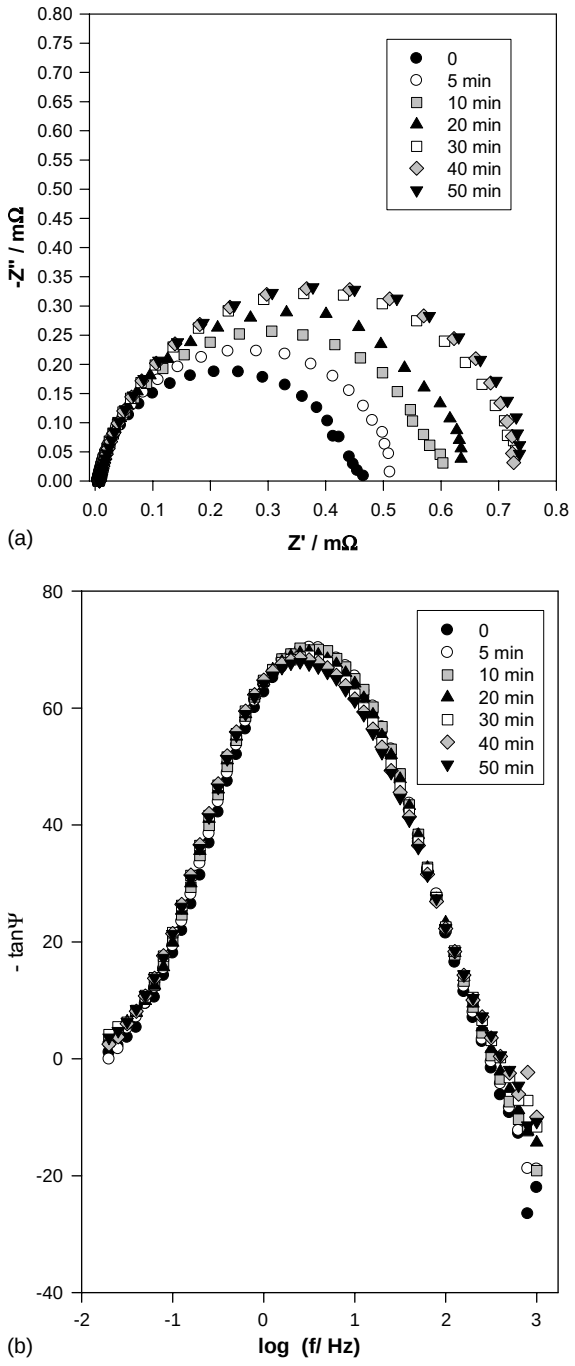

Fig. 8. (a) Effect of interruption of the cathodic humidification on the Nyquist plots at V_{bias} = 4.5 V (initial state ChAd). Frequency range 1 kHz–0.01 Hz. Legend indicates the time after cutting off the humidification. (b) Effect of interruption of the cathodic humidification on the Bode plots (phase angle Ψ as a function of frequency) at V_{bias} = 4.5 V. Initial state ChAd. Legend indicates the time after cutting off the humidification.

$$(r_p^o)_{app} = \frac{RT}{nF(i^o)_{app}} \tag{13}$$

From Equations 12 and 13 it appears that the observed increase of R'_p following the interruption of humidification provides a measure of the apparent activity decrease of the cathode. In principle, this decrease may be due to a decrease in the intrinsic activity of the electrode, i^o, or to a decrease in the electrocatalytically active surface area S_{act} (the actual area of the catalyst corresponding to 1 cm^2 geometrical area)

$$(i^o)_{app} = i^o S_{act} \tag{14}$$

To decide between the two options, we examined the behaviour of the Bode plots (phase angle vs frequency). These plots are expected to be identical if the only change in the system is a variation of the surface (since the two components of the impedance (Z and Z') are affected in the same proportion). An inspection of the Bode plots in Figure 8(b) shows that, despite the significant changes in R'_p, the phase angle is practically constant during the experiment. This observation supports the idea that the change occurring during the dehydration is a decrease in S_{act}. Other causes for the decrease in double layer capacitance can be ascribed, like the change of the dielectric properties of the double layer, to dehydration. However, if this were the case, the phase angle would change with respect to the initial value.

Approximate values of the latter can be obtained from the double layer capacity of the cathode (C_{dl}) by dividing by the capacitance of 1 cm^2 of Pt at 0.9 V vs NHE, that is, $C_{dl}(Pt)$ = 40 μF cm^{-2} [19]. To avoid errors introduced by the choice of C_{dl} (Pt), we have represented in Figure 9 only the relative changes in time of the ratio S_{act} (t)/S_{act} (0) = C_{dl} (t)/C_{dl} (0).

The fact that the effect of the cathode humidification removal is equivalent to a decrease in active surface area of the electrocatalyst can be explained in terms of the dehydration of the Nafion present in the catalytic layer. Here, the role of Nafion is to insure continuity of the proton paths between the membrane and the catalytic sites. Dehydration can produce an interruption of some of those paths, which is equivalent to the disappearance of part of the active sites.

Although $\Delta R'_p$ data, obtained from potentiostatic EIS experiments cannot be directly compared with the values ΔR_p obtained from galvanostatic transients, it is reasonable to assume that the origin of the deactivation due to a decreased water exposure is the same.

Thus, it appears that the effects of membrane conductivity changes due to dehydration have been largely overestimated in the past and that most of the performance loss observed originates in the cathode catalytic layer. This idea is supported by recent studies, demonstrating the positive effect of hydrophilic agents added to the catalytic layer on the performance of fuel cells operated at high temperatures or in the absence of cathode humidification [20].

4. Conclusions

The *in situ* ohmic resistance of thin (30 μm) Nafion membranes in Gore Primea 5561 MEAs was determined

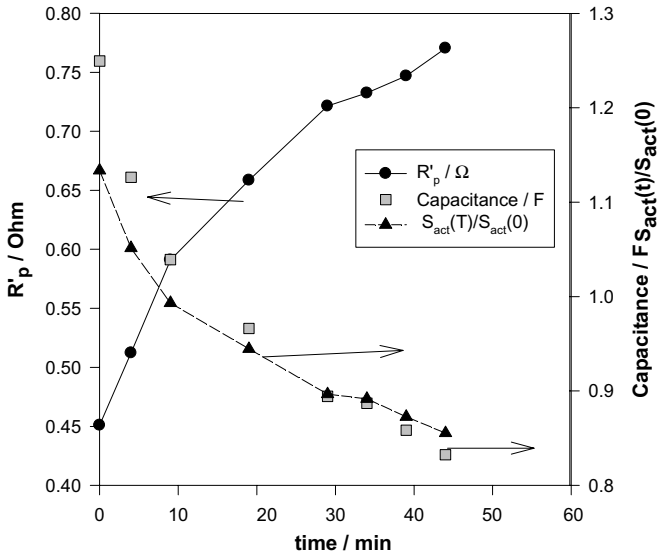

Fig. 9. Change of R'_p, C_{dl} and $S_{act}(t)/S_{act}(0)$ as a function of time after interruption of the cathodic humidification (Initial state ChAd).

at current densities in the 0–400 mA cm^{-2} range and different humidification conditions. Two different types of current dependencies were found, depending on whether the cathode was humidified or not. For the stack with cathodic humidification (cases ChAh or ChAd), the membrane resistance was found to be practically constant, no matter whether the anode was humidified or not. This behavior is similar with that reported by Slade for fully humidified membranes of Nation 112 [13]. For the stack with non-humidified cathodes, the membrane resistance was considerably higher at low current and showed a decrease with increasing current, more significant for the system with anodic humidification (CdAh); for the latter, the values at the upper limit of the investigated current range were close to those obtained for the fully humidified stack. The decrease in membrane resistance with increasing current for the case CdAh is similar to that reported by Watanabe et al. for very thin membranes of recast Nafion [17] and can be explained in terms of the current dependence of the effective drag coefficient [18].

The resistance transients after the interruption of humidification also show a significant dependence on the humidification type: the increase in membrane resistance Δr_m is significant after interruption of the cathodic humidification (no matter whether the anode is still humidified or not) and relatively small after interrupting the anode humidification. Thus, the change in resistance appears to be determined by the water concentration c_o at the cathode/membrane interface. Significant changes appear to be due to a reequilibration of the water profile in the membrane from a state with a constant c_o (as determined by the presence of liquid water in the cathode compartment) to one in which c_o is small and current-dependent. This reequilibration is rate-determining for the observed resistance increase after the interruption of cathode humidification.

The most important conclusion is that the increase in membrane resistance is responsible only for a relatively small part of the voltage decay observed after removing the cathode humidification. To account for the voltage decrease in excess to that caused by membrane dehydration, an additional resistive contribution had to be considered, which shows a current dependence similar with that of the ohmic resistance of the membrane. Based on data obtained from EIS experiments, this contribution was assigned to an increase in the polarization resistance, caused by the dehydration of the Nafion in the catalytic layer of the cathode. The apparent deactivation of the cathode produced by dehydration was tentatively explained by a decrease in the active surface area of the electrocatalyst, as a result of the latter process.

References

1. T.A. Zawodzinski, C. Derouin, S. Radzinski, R.J. Sherman, V.T. Smith, T.E. Springer and S. Gottesfeld, *J. Electrochem. Soc.* **140** (1993) 1041.
2. J.T. Hinatsu, M. Mizuhata and H. Takenada, *J. Electrochem. Soc.* **141** (1994) 1493.
3. T.A. Zawodzinski, T.E. Springer, J. Davey, R. Jestel, C. Lopez, J. Valerio and S. Gottesfeld, *J. Electrochem. Soc.* **140** (1993) 1981.
4. M.W. Verbrugge and R.F. Hill, *J. Electrochem. Soc.* **137** (1990) 3770.
5. V.A. Paganin, C.L.F. Oliveira, E.A. Ticianelli, T.E. Springer and E.R. Gonzalez, *Electrochim. Acta* **43** (1998) 3761.
6. T. Okada, G. Xie and Y. Tanabe, *J. Electroanal. Chem.* **413** (1996) 49.
7. T.E. Springer, T.A. Zawodzinski and S. Gottesfeld, *J. Electrochem. Soc.* **138** (1991) 2334.
8. K. Dannenberg, P. Ekdunge and G. Lindbergh, *J. Appl. Electrochem.* **30** (2000) 1377.
9. D.R. Sena, E.A. Ticianelli, V.A. Paganin and E.R. Gonzalez, *J. Electroanal. Chem.* **477** (1999) 164.
10. G.J.M. Jansen and M.L.J. Overvelde, *J. Power Sources* **101** (2001) 117; R.J. Bellows, M.Y. Lin, M. Arif, A.K. Thompson and D. Jacobson, *J. Electrochem. Soc.* **146** (1999) 1099.

11. T.A. Zawodizinski, M. Neeman, L.O. Sillerud and S. Gottesfeld, *J. Phys. Chem.* **95** (1991) 1040.
12. P.C. Reike and N.E. Vanderborgh, *J. Membr. Sci.* **32** (1987) 313.
13. S. Slade, S.A. Campbell, T.R. Ralph and F.C. Walsh, *J. Electrochem. Soc.* **149** (2002) A 1556.
14. F.N. Buchi and G.G. Scherer, *J. Electroanal. Chem.* **404** (1996) 37.
15. F.N. Buchi and G.G. Scherer, *J. Electrochem. Soc.* **148** (2001) A 183.
16. A. Paganin, E.A. Ticianelli and E.R. Gonzalez, *in* S. Gottesfeld, G. Halpert and A. Landgrebe (Eds) 'Proton Conducting Membrane Fuel Cells', PV 95-23, The Electrochem. Soc. Proceedings Series (Pennington, NJ, 1995), p. 102.
17. M. Watanabe, H. Igarashi, H. Uchida and F. Hirashawa, *J. Electroanal. Chem.* **399** (1995) 239.
18. M. Ciureanu and M. Badita, *J. New Mat. Electrochem. Syst.* in press.
19. M. Ciureanu and R. Roberge, *J. Phys. Chem.* **105**, (2001) 3531.
20. C. Hawk, A. Smirnova, J.M. Fenton and H.R. Kunk, Proceedings of the 200th Meeting of the Electrochemical Society, San Francisco, 2–7 Sept. (2001), Abstr. 424.